The Chemist
Journal of the American Institute of Chemists

Adsorptive Removal of Congo Red Dye by a Synthesized Dual Ligand (Carboxylate and N-donor) Coordination Compound

V. O. Adimula [a*], R. A. Anifowose [a], E. O. Adeniyi [a], A. D. Obafemi [a], S. E. Elaigwu [b], S. Owalude [b], A. C. Tella [b]

[a] *Department of Industrial Chemistry, University of Ilorin, Ilorin, Nigeria*
[b] *Department of Chemistry, University of Ilorin, Ilorin, Nigeria*

**Corresponding author (E-mail: vincentadimula@gmail.com; Tel: +2348036973282)*

Abstract: The adsorption of Congo red dye from water by a synthesized Cu(II) coordination compound formulated as [Cu(BTCA)(AMB)] is herein reported (BTCA= 1,2,4,5-bezene tetra carboxylic acid; AMB= 4-aminomethylbenzoic acid). Characterization of the compound was achieved by X-ray diffraction (XRD), Fourier-transform infrared (FTIR) spectroscopy, scanning electron microscopy (SEM), and thermogravimetric analysis (TGA). The adsorption performance of the compound was assessed through batch adsorption experiments. Kinetic and isotherm models were employed to elucidate the adsorption mechanism and establish a comprehensive understanding of the interaction between the compound and Congo red dye molecules. The SEM analysis results before and after adsorption showed the presence of the dye molecules on the adsorbent. Adsorption data were seen to be best for the pseudo-second order kinetics model. Thermodynamic parameters indicated that the adsorption process is spontaneous by ΔG values ranging from -0.38 KJ/mol to -2.15 KJ/mol.

Key Words: coordination compound, adsorption, Congo red dye, characterization, pseudo second order

1. Introduction

Coordination polymers have been noted to be a group of functional materials that have found applications in multiple processes. The study of coordination polymers has expanded rapidly in the past decade due to its susceptibility to attain a variety of architectures built up from an extended range of molecular building blocks with varying interactions. Coordination compounds with backbones, constructed from metal ions as connectors

and ligands as linkers, have been utilized in various processes due to their interesting characteristics [1]. Coordination networks having porous features have advanced nanoporous compounds for processes, which include catalysis, adsorption, and gas separation, among others, due to their tunable pore sizes, large surface areas, high porosities, and good thermal and mechanical stabilities [2,3].

The study of coordination compounds involves the study of metals, which perform a variety of roles in many biological, catalytic, and materials applications and are essential parts of coordination chemistry. To harness their reactivity and fully utilize their potential in various domains, it is crucial to comprehend the behavior and characteristics of metal centers in coordination compounds [3]. Their electrical structure determines the bonding and reactivity of metal centers. Metal ions frequently display varying oxidation states which cause coordination compounds to develop with various electronic configurations [4]. The stability and spectroscopic characteristics of metal complexes are influenced by the distribution of electrons in the metal d orbitals [5]. Specific coordination geometries, such as octahedral, square planar, or tetrahedral, are adopted by metal centers in coordination complexes. These geometries are determined by the type of ligands used and the metal ion's electronic state [3].

Dyes, such as Congo red, are reportedly utilized as coloring agents for materials such as leather, textile, and paper, among others [5-7]. The reactiveness of some dyes makes them suitable for use due to their brightness and fastness when used [4,5]. These dyes, however, present the problem of toxicity and carcinogenicity when used, causing harm directly to aquatic life and humans, thus, generating conditions that include lung cancer and neurological disorders. The removal of these toxins from the environment is hindered by the structural complexity of synthetic dyes and their highly water-soluble nature [7-9].

We herein report the sorption of Congo red dye from water by a synthesized Cu(II) complex containing mixed 1,2,4,5-bezene tetra carboxylic acid (BTCA) and 4-aminomethyl benzoic acid (AMB) ligands, as adsorbents for the removal of Congo red dye from aqueous solution. The compound was successfully characterized and formulated as [Cu(BTCA)(AMB)].

2. Experimental

Materials and Methods

The reagents used for this study were of analytical grade and used without further purification. The absorbance measurements were taken using a SHIMADZU UV-1650 UV-Vis spectrophotometer. Scanning electron microscopy (SEM) was carried out using a JEOL JSM-7600F Scanning Electron Microscope.

Synthesis of the [Cu(BTCA)(AMB)]

The compound was synthesized using a solvent-based method. Solutions of the ligands (BTCA and AMB; 1 mmol each) were dissolved in 10 mL each of dimethyl

formamide and distilled water separately and transferred into a round-bottom flask containing the dissolved Cu^{2+} salt. The mixture was stirred thoroughly to ensure homogeneity and refluxed for 2 h at 120°C with constant stirring. The precipitate formed was thereafter isolated by filtration, washed with 50:50 DMF and distilled water, dried, and stored.

Batch Adsorption Studies

Adsorption of Congo red (CR) dye onto [Cu(BTCA)(AMB)] was studied using a Congo red stock solution of 1000 mg/L. This was prepared by dissolving 0.25 g of the Congo red dye in 250 ml of deionized water. Absorbance of the Congo red solution was then observed using a UV-Visible spectrophotometer to obtain the wavelength of maximum absorption which was found to be 500 nm. Lower concentrations of the dye (5–30 mg/L) were prepared from the stock solution by serial dilution with deionized water and absorbance readings taken with the UV–Visible spectrophotometer at a λ_{max} value of 500 nm [6]. The graph of absorbance against concentration was plotted to give the calibration curve (Figure 1).

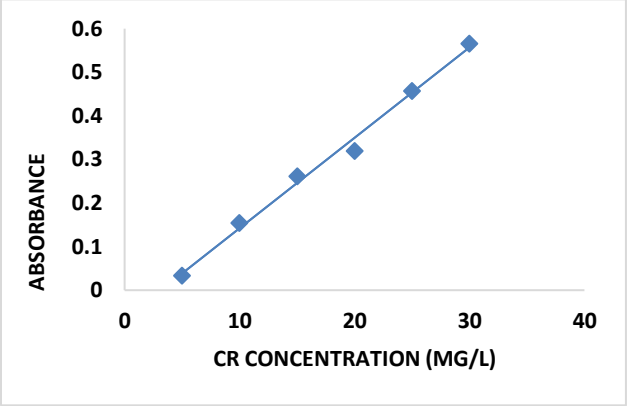

Figure 1. Calibration Curve for Congo Red Dye Adsorption onto [Cu(BTCA)(AMB)]

The effect of concentration, temperature, time, pH, and the dose of adsorbent on the adsorption process was investigated. To determine the quantity adsorbed (q_e in mg/g) at equilibrium, equation 1 was utilized:

$$q_e = \left(\frac{C_o - C_e}{m}\right) v \quad (1)$$

where Co and Ce (mg/L) are the initial and final concentrations of the adsorbates, respectively, v is the volume of the solution used (L), and m is the mass (g) of the adsorbents.

The effect of concentration was studied using 5–30 mg/L of the adsorbate, while the effect of temperature was studied at the temperature range of 30–70°C. The effect of pH was investigated by varying the pH between 2 and 13 using 0.1 M HCl or 0.1 M NaOH, while the effect of adsorbent dosage was studied using 0.01–0.05 g of the adsorbents, and the investigation of effect of time was done at time interval of 60–300 min [7].

3. Result and Discussion

Result of SEM Analysis

Figure 2a and 2b depict the SEM images of [Cu(BTCA)(AMD)] before and after adsorption.

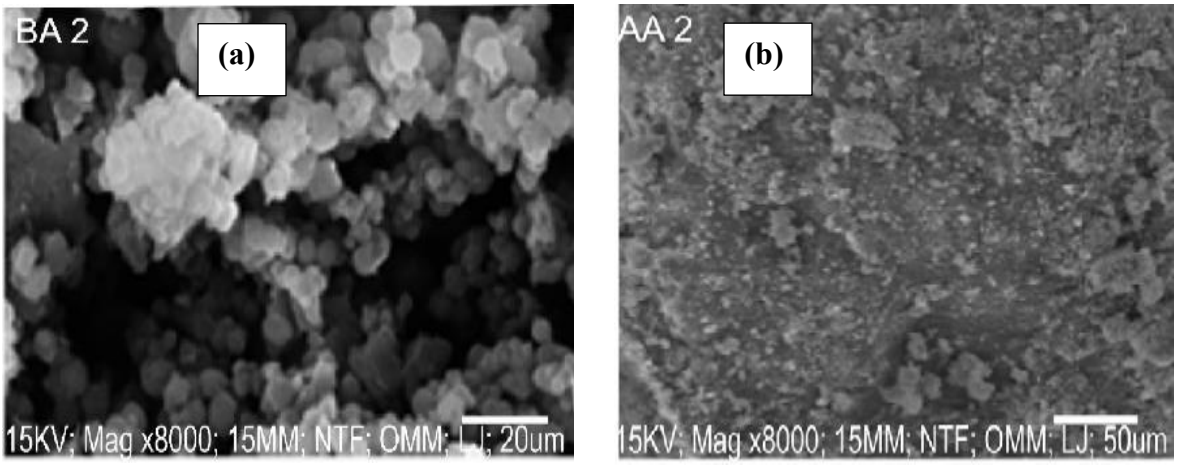

Figure 2. SEM Images of [Cu(BTCA)(AMD)] a) Before Adsorption; b) After Adsorption

The surface morphology showed the presence of voids in-between the particles before adsorption while the image after adsorption shows the incorporation of the dye into the voids in-between the particles (Figure 2b).

Result of PXRD Analysis

The PXRD pattern of the [Cu(BTCA)-(AMD)] compound, before and after adsorption, are presented in Figure 3 (a and b).

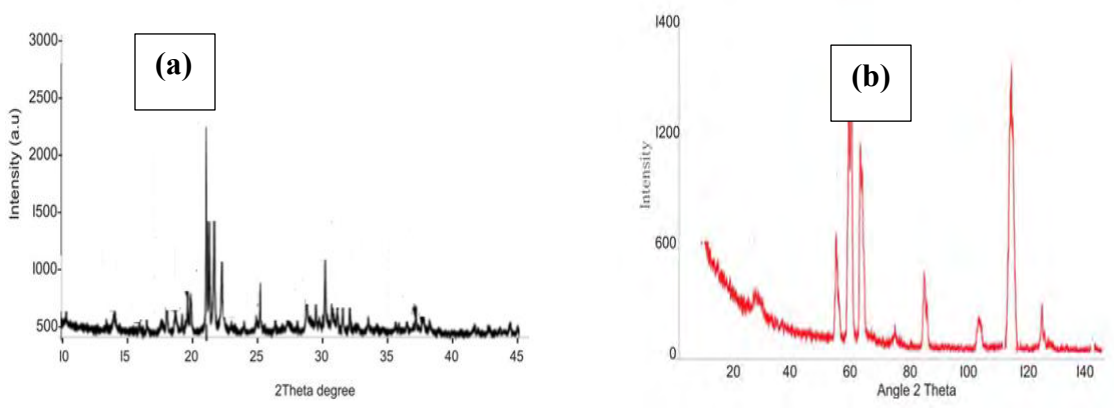

Figure 3. PXRD Analysis Result of a) Before Adsorption; b) After Adsorption

A comparison of the patterns showed a reduction in intensity of peaks generally for the PXRD pattern after adsorption of CR dye. This is attributed to the presence of the dye molecules on the adsorbent [8-10].

Result of TGA Analysis

The TGA of the compound showed two stages of decomposition within a temperature range of 0–650°C [9-11]. The first stage of decomposition results to about 12% weight loss, ranging from a temperature of 0–290°C. The second decomposition stage, which starts from 290°C and ends at 500°C, results in a weight loss of 79%. Figure 4 shows the TGA curve of the sample.

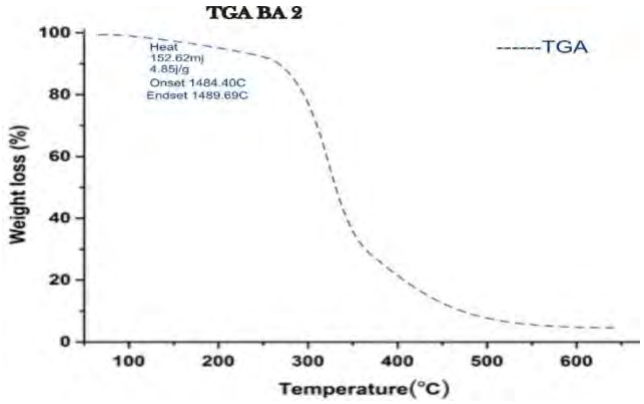

Figure 4. TGA Curve of [Cu(BTCA)(AMD)]

Result of FTIR Analysis

Using a Shimadzu FTIR spectrophotometer, the functional groups present in the [Cu(BTCA)(AMD)] compound, before and after adsorption, were obtained by studying the spectral as shown in Figure 5. Peaks observed at 3496.99 cm^{-1} and 3444.96 cm^{-1} were attributed to the presence of hydroxyl (O-H) and amino group (N-H), respectively. The peak observed at 1710 cm^{-1} was attributed to the carbonyl group of the carboxylate. The diagnostic region of the compound, before and after adsorption, were observed to be similar. However, the presence of the Congo red dye on the compound, after adsorption, causes a significant difference in the fingerprint region (Figure 5, a and b).

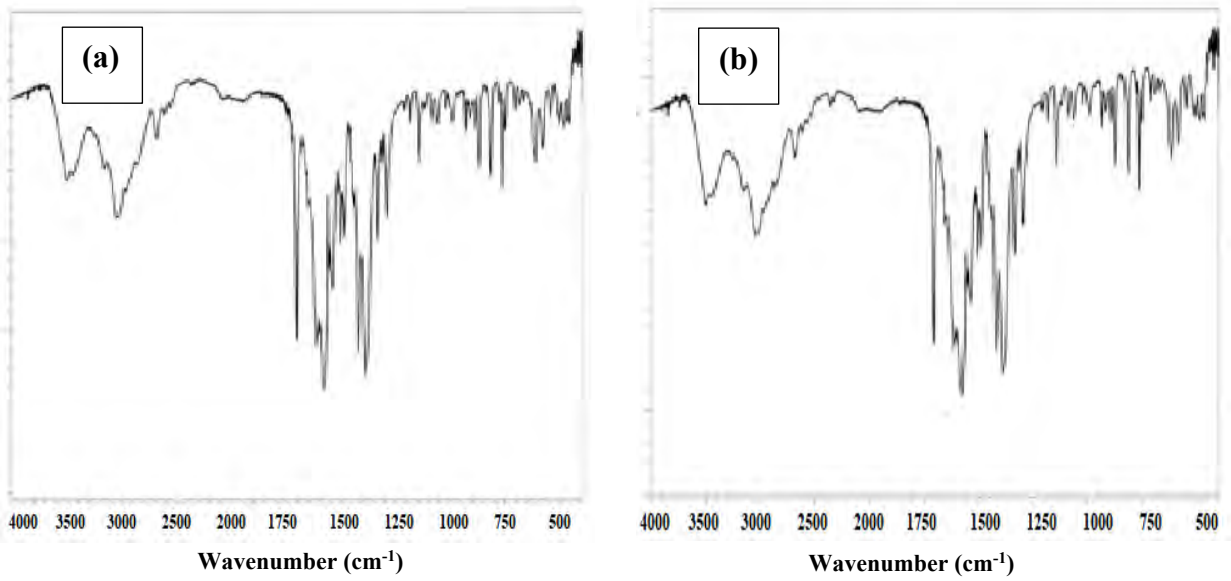

Figure 5. FTIR Spectroscopy Analysis of [Cu(BTCA)(AMB)] a) Before Adsorption; b) After

The peak observed at 732 cm^{-1} in the spectra after adsorption was attributed to the characteristic FTIR band of the ν(S-O) group in the Congo red dye. This peak was observed to be absent in the spectra before adsorption study.

Adsorption Study

Effect of Congo Red Dye Concentration

The findings from investigating the effect of Congo red dye concentration on the adsorption process using the adsorbents is presented in Figure 6.

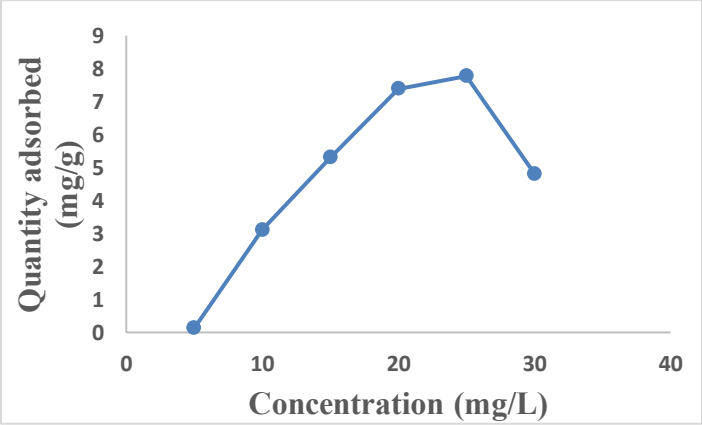

Figure 6. Effect of Concentration on the Adsorption of Congo Red Dye by [Cu(BTCA)(AMB)]

It was observed that as the concentration of the dye increased, the amount of Congo red dye adsorbed onto the adsorbents also increased, reaching its maximum at 25 mg/L. As the dye concentration increased, the adsorption sites on the adsorbents became saturated, resulting in the subsequent release of the dye as the process continued. This phenomenon occurred because there was intensified competition among Congo red dye molecules for the available adsorption sites on the adsorbent, causing an initial surge in the adsorption rate, followed by a gradual deceleration of the process. This behavior can be attributed to the fact that at lower dye concentrations, there is a higher ratio of solute to vacant adsorbent sites, leading to increased quantity adsorbed [8].

Effect of Time

The impact of time on the adsorption of Congo red dye onto the [Cu(BTCA)(AMB)] material, as presented in Figure 7, suggests that as the contact time increased, the efficiency of adsorption gradually rose and reached its maximum value after 120 minutes, after which it remained constant.

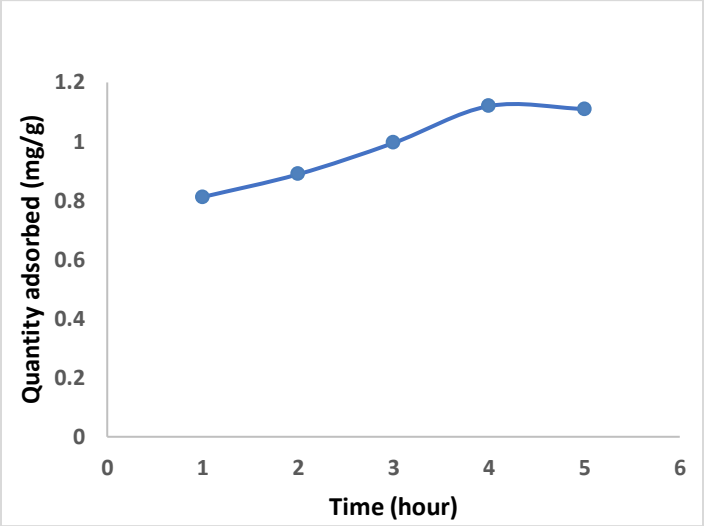

Figure 7. Effect of Time on the Quantity of Congo Red Dye Adsorbed

This experiment was conducted at a pH of 7.0 with a dye concentration of 25 mg/L. A dosage of 0.01 g of adsorbent was used for durations ranging from 60 to 360 minutes to determine the equilibrium time for the adsorption process. The initial increase in adsorption is attributed to the presence of available adsorption sites on the materials, which gradually became occupied over time [9-12].

Effect of pH

The impact of change in pH on the adsorption of Congo red dye by [Cu(BTCA)(AMB)] is presented in Figure 8. Equilibrium concentrations of dye at 25 mg/L over 240 min were employed. Adjusting the pH within the range of 2.0 to 11.0 using either 0.1 M HCl or 0.1 M NaOH [9] indicated that at lower pH (between 3.0 and 6.0), sorption of Congo red dye onto [Cu(BTCA)(AMB)] decreases.

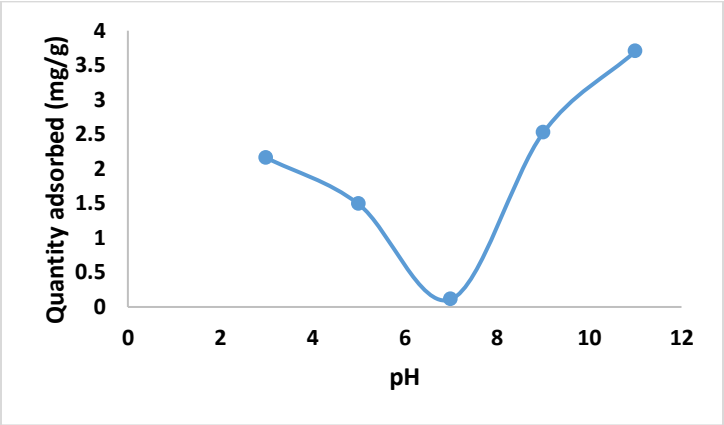

Figure 8. Effect of pH on the Quantity of Congo Red Adsorbed

This phenomenon is attributed to an acid-base interaction between the dye molecules and the surface of the [Cu(BTCA)(AMB)]. Conversely, at higher pH values (ranging from 8.0 to 12.0), the Congo red dye adopts an anionic nature due to the presence of hydroxyl ions in its solution. This leads to an increased adsorption of the dye onto the surface of the adsorbent [9,13,14].

Effect of Temperature

The effect of temperature change on the adsorption process was monitored using 0.01 g of the adsorbent for this study. The temperature was varied within the range of 30 to 70°C, and each experiment lasted for 4 hours.

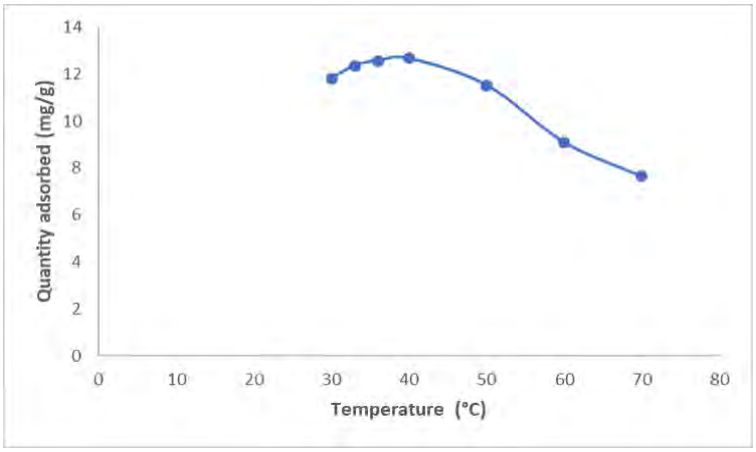

Figure 9. Effect of Temperature on the Quantity of Congo Red Dye Adsorbed

The findings presented in Figure 9 revealed that the quantity adsorbed increases after an increase in the temperature to 40°C and later decreases at a further increase in temperature. The decline in quantity adsorbed may be attributed to the increased kinetic energy acquired by the dye molecules at temperatures beyond 40°C [15-17].

Effect of Adsorbent Dose

The impact of varying the dosage of adsorbents on the adsorption of Congo red dye was examined in this study (Figure 10). Specifically, a constant equilibrium dye concentration of 25 mg/L was maintained, and the study was done at a temperature of 40°C.

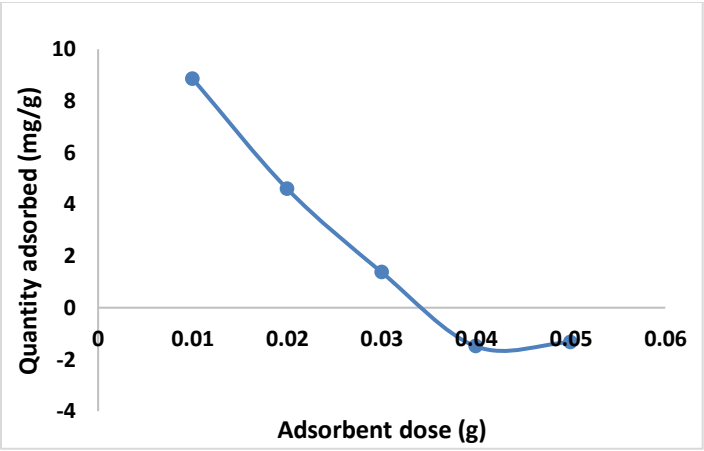

Figure 10. Effect of Adsorbent Dose on the Quantity of Congo Red Adsorbed on the Adsorbents

The quantity of adsorbent used in the experiment was adjusted, ranging from 0.01 to 0.05 g. It was observed that as the amount of adsorbent increased, the quantity adsorbed

decreased. This can be attributed to an agglomeration of the adsorbent particles due to the increased quantity of adsorbents employed [10,14,18].

Adsorption Isotherms Studies

To assess the adsorption of congo red dye over [Cu(BTCA)(AMB)], three different models, Langmuir, Freundlich, and Temkin, were employed in an effort to determine which isotherm model best describes the adsorption process [8]. The parameters obtained from subjecting the adsorption data to the various isotherm models are given in Table 1.

Table 1. Isotherm Parameters for Congo Red Dye Adsorption on [Cu(BTCA)(AMB)]

Isotherms	Equation	Constants	Values
Langmuir	$\frac{Ce}{qe} = \frac{1}{KaQm} + \frac{Ce}{Qm}$	Qm (mg g^{-1})	-0.693
		ka	-0.09
	$R_l = \frac{1}{1 + KaCo}$	R_L	0.8
		R^2	0.116
Freundlich	$\ln qe = \ln K_f + \frac{1}{n} lnCe$	K_f	0.089
		n	0.635
		R^2	0.359
Temkin	$\mathrm{Qe} = \mathrm{BlnA} + \mathrm{BlnCe}$	A	0.553
		B	2.930
		R^2	0.9487

The Langmuir adsorption isotherm (equation 2) was studied by plotting a graph of Ce/Qe against

$$\frac{Ce}{qe} = \frac{1}{KaQm} + \frac{Ce}{Qm} \quad (2)$$

Ce (Figure 11), where Ce is the final concentration, and Qe is the quantity of Congo red adsorbed.

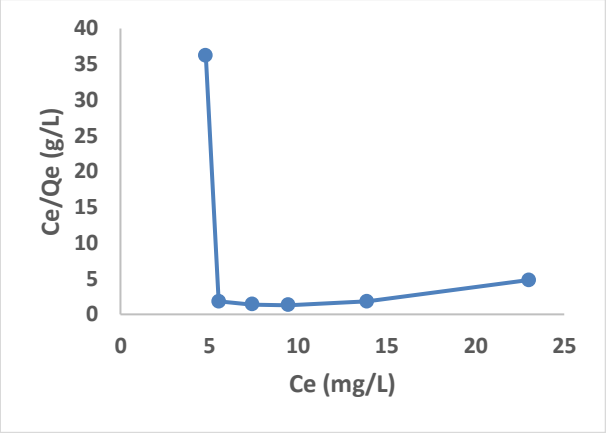

Figure 11. Langmuir Isotherm Model Plot for the Adsorption of Congo Red Dye by [Cu(BTCA)(AMB)]

The linear form of the Langmuir isotherm model gave the values of Ka [the Langmuir adsorption constant (L/mg)] and Qm [theoretical maximum adsorption capacity (mg/g)] obtained from the intercept and slope of the plot of the graph [9]. Adsorption is speculated to be a monolayer adsorption with no interaction between the adsorbate molecules.

The linear form of the Langmuir model and the equation used in calculating the separation factor (R_L) (equation 3) are given in equations below:

$$R_l = \frac{1}{1+KaCo} \tag{3}$$

where Ka (L/mg) is the Langmuir constant, and Co (mg/L) is the initial concentration. The adsorption process can be determined as favorable when the R_L value lies between 0 and 1. The Qm value was found to be -0.6922 and the constant Ka to be -0.09. The R_L was calculated to be -0.8, which falls below 0 and indicates unfavorable adsorption, while the R^2 value was obtained as 0.1166.

The relationship of the amount adsorbed per unit mass or mole with concentration is demonstrated by the Freundlich model (equation 4) given as:

$$\ln qe = \ln K_f + \frac{1}{n} lnCe \tag{4}$$

The Freundlich isotherm model parameters such as the 1/n and as K_f [(mg g^{-1})/(mg L^{-1})] were obtained from the intercept and slope of the linear plot of lnQe versus ln Ce (Figure 12), respectively.

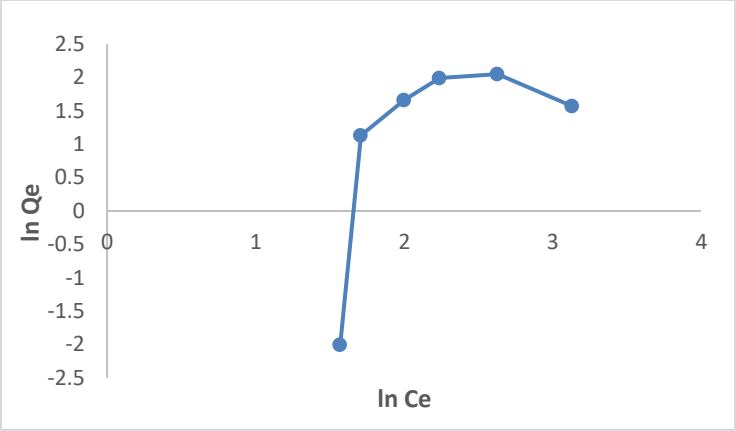

Figure 12. Freundlich Isotherm Model Plot

The K_f, Freundlich constant is the adsorption capacity, that is the adsorptive power, and the 1/n, heterogeneity factor, indicates the energy of adsorption. The 1/n value of 1.527 obtained indicates the unfavorable adsorption of Congo red dye for adsorption onto the adsorbents, while lower R^2 value of 0.359 for the adsorbents indicates that the Freundlich model less fits the experimental data

The Temkin isotherm model (equation 5) was used to estimate the heat of the adsorption and the adsorbent–adsorbate interaction.

$$Q_e = BlnA + BlnC_e \quad (5)$$

It is evaluated using the equation given below by plotting the graph of Qe against ln Ce (Figure 13), and the constants A (g/L) and B (J/mole) corresponding to the maximal equilibrium binding energy and heat of adsorption, respectively, were calculated using the linearized Temkin equation.

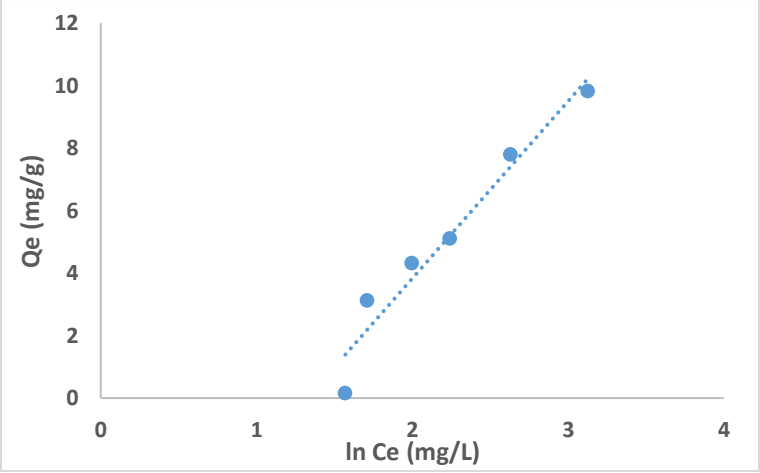

Figure 13. Plot of Temkin Isotherm Model

The obtained values of A and B are given as 0.553 and 2.930, respectively. The R^2 value of 0.9487 obtained indicated the best-fit of the Temkin adsorption isotherm to the adsorption data obtained for uptake of Congo red dye by [Cu(BTCA)(AMB)]. This suggests the occurrence of adsorbent–adsorbate interactions in the adsorption process [16].

Adsorption Kinetics

The experimental adsorption data for the adsorption of Congo red dye by [Cu(BTCA)(AMB)] was analyzed using the kinetic models of pseudo-first order, pseudo-second order, intraparticle diffusion model and Elovich diffusion model. Parameters obtained were summarized in Table 2.

Table 2. Kinetic Parameters for Congo Red Adsorption by [Cu(BTCA)(AMB)]

Models	Equations	Parameters	values
Pseudo-first order	$\ln(q_e - q_t) = \ln(q_e) - K_1 t$	k_1	0.0091
		q_e (cal)	0.79
		R^2	0.748
Pseudo-second order	$\frac{t}{q_t} = \frac{1}{K_2\, q_e^2} + (\frac{1}{q_e})t$	K_2	0.018
		q_e (cal)	1.25
		R^2	0.99
Intra-particle diffusion	$q_t = K_{idiff}\, t^{1/2} + C$	C	0.5318
		K_{idiff}	0.0349
		R^2	0.949
Elovich	$q_t = \frac{1}{\beta}\ln(\alpha\beta) + \frac{1}{\beta}\ln(t)$	B	4.87
		R^2	0.9389

Pseudo First Order Kinetics (Lagergren Model)

The Lagergren model (equation 6) parameters for the uptake of Congo red dye by the [Cu(BTCA)(AMB)] absorbent was derived by plotting ln ($q_e - q_t$) against time from the linearized form of the equation given below.

$$\ln (q_e - q_t) = \ln(q_e) - K_1 t \quad (6)$$

Values of k_1 and q_e were determined from the slope and intercept. The q_e value was obtained as 0.79, and k_1 was obtained as 0.0091. The discrepancy between the intercept and the actual experimental Qe value signifies that this model does not accurately describe the experimental data, indicating that the adsorption rate does not conform to this equation [16].

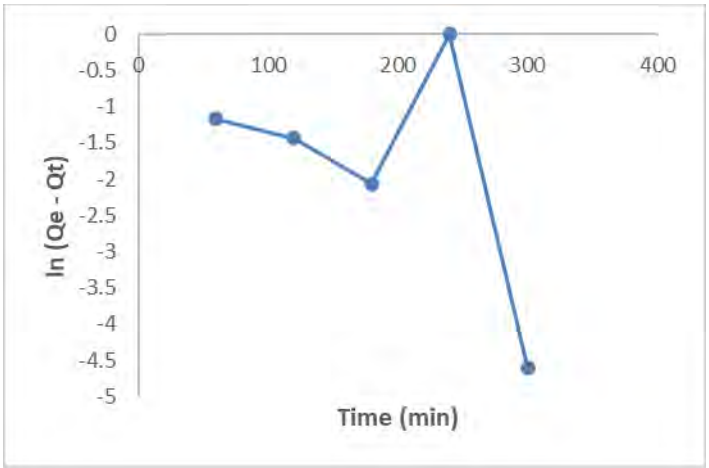

Figure 14. Pseudo First Order Kinetics Plot for Congo Red Adsorption by [Cu(BTCA)(AMB)]

Pseudo-Second Order Kinetic Model

The adsorption data for uptake experiment of Congo red dye by [Cu(BTCA)(AMB)] was analyzed using the pseudo-second-order kinetic model. A linear relationship was observed from the plot t/Qt versus t (Figure 15), exhibiting a notably strong correlation coefficient (R^2) value.

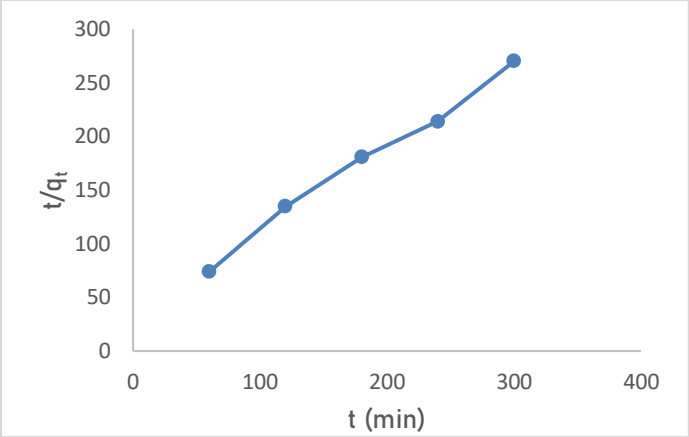

Figure 15. Pseudo-Second Order Kinetics Plot for Congo Red Adsorption by [Cu(BTCA)(AMB)]

Both the equilibrium adsorption capacity (Qe) and the rate constant (k_2) were computed by extracting these values from the slope and intercept, respectively. The Qe and k_2 values were calculated to be 1.27 and 0.018, respectively. The pseudo-second-order model proves its applicability to the adsorption experiment due to the high correlation coefficient (R^2) value of 0.99 obtained, and also indicates it best explains the adsorption process [17]. The linearized form of the pseudo-second order rate equation (7) is given as:

$$\frac{t}{q_t} = \frac{1}{K_2\, q_e^2} + \left(\frac{1}{q_e}\right)t \tag{7}$$

Intraparticle Diffusion Model

The intraparticle diffusion model is often represented by a plot of the amount of adsorbate adsorbed (Qt) against the square root of time ($t^{1/2}$) using the equation (8) below:

$$q_t = K_{idiff}\, t^{1/2} + C \tag{8}$$

The values of K_{diff} [the intraparticle diffusion rate constant ($mg/g/min^{1/2}$)] and C (thickness of the boundary layer) were calculated from the slope and intercept of the plot of q_t versus $t^{1/2}$ (Figure 16) and obtained as 0.0349 and 0.5318, respectively. The R^2 value was found to be 0.949 which indicates that the experimental data can be explained by the intraparticle diffusion adsorption kinetics model [15,16].

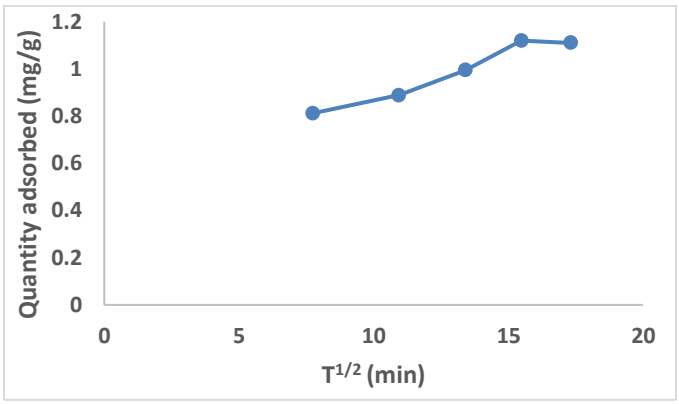

Figure 16. Intraparticle Diffusion Model Plot

Elovich Kinetics Model

The adsorption of Congo red onto the adsorbent surfaces was analyzed using the Elovich model. This model accounts for the non-linear behavior that is frequently seen during the early phases of adsorption. The Elovich equation, plot of q_t against ln(t), presented a slope of (1/ β) and an intercept of (1/β) ln (αβ). The value of β was calculated to be 4.87, and α to be 0.16 (Figure 17).

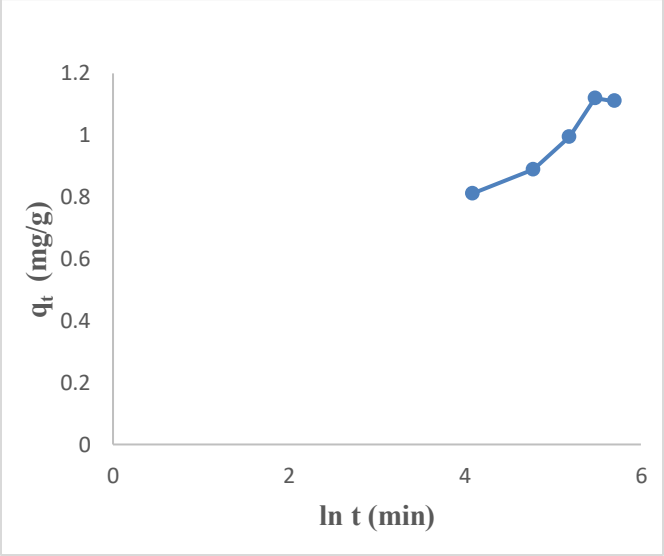

Figure 17. Elovich Kinetic Model Plot

However, it's worth noting that the correlation coefficients (R^2) were found to be high with a value of 0.9389, indicating that this model is suitable for an assessment of the

adsorption process [17]. The linearized equation (9) for the Elovich kinetic model is given as:

$$q_t = \frac{1}{\beta}\ln(\alpha\beta) + \frac{1}{\beta}\ln(t) \quad (9)$$

The data presented in Table 2 suggests that the Congo red dye adsorption experiment best-fits the pseudo-second-order kinetics with a correlation coefficient value of 0.99. This fit was superior compared to alternative kinetic models across the entire adsorption process. Consequently, it can be inferred that the pseudo-second-order equation provides a more accurate description of the adsorption kinetics of Congo red dye on the adsorbent. This suggests that occurrence of chemical interaction between the adsorbate and the adsorbent as suggested by the Temkin isotherm model earlier analyzed [14,16,18-20].

Adsorption Thermodynamics

To obtain the thermodynamics data of the adsorption study of Congo red dye on the adsorbent, an investigation of the thermodynamics was done at five different temperatures ranging from 30° to 70°C. The change in Gibbs free energy (ΔG°), change in entropy (ΔS°) and change in enthalpy (ΔH°) were calculated based on the equations 10, 11 & 12 [11]:

$$K_c = \frac{C_a}{C_e} \quad (10)$$

$$\Delta G = \Delta H - T\Delta S \quad (11)$$

$$\text{Log Kc} = \frac{\Delta S}{2{:}303 \text{ x R}} - \frac{\Delta H}{2{:}303 \text{ x R x T}} \quad (12)$$

In the equations above, Kc is the equilibrium constant, Ca and Ce represent the quantity of Congo red dye adsorbed on the adsorbent and the final concentration of the solution, respectively. T is the temperature in kelvin and R= molar gas constant which is 8.314 J $K^{-1}mol^{-1}$.

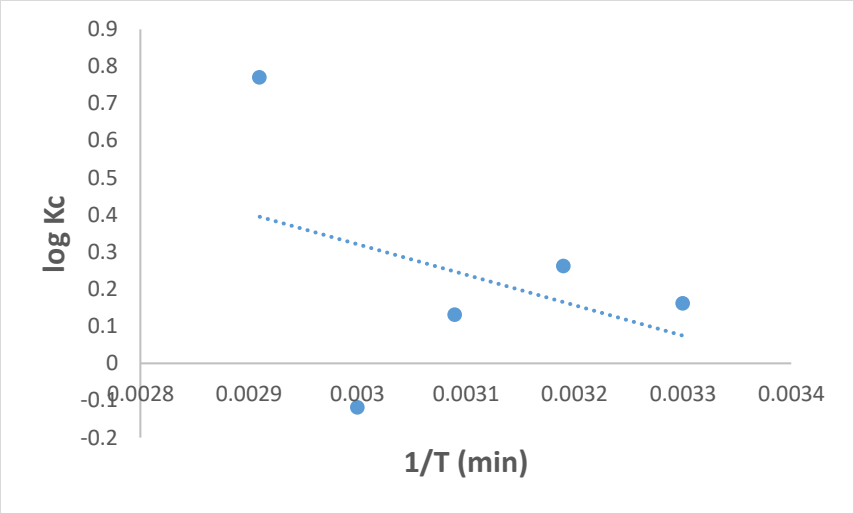

Figure 18. Thermodynamic Plot for Congo Red Dye Adsorption by [Cu(BTCA)(AMB)]

The Gibbs free energy change (ΔG°) values for the adsorption experiment at different temperatures were obtained as negative values (Table 3), indicating that the sorption process was spontaneous [13,15]. The change in enthalpy value calculated was obtained as 15.721 KJ/mol, and the change in entropy was 53.15 J/mol. The positive value of these two thermodynamic parameters depicts an endothermic process [13]. Since the range of the free energy is less than 20 KJ/mol, the thermodynamic investigation could be concluded as a physical sorption process which is spontaneous and endothermic [9,11].

Table 3. Thermodynamic Parameters for Congo Red Dye Adsorptions on to [Cu(BTCA)(AMB)]

Temperature (K)	ΔG° (KJ/mol)	ΔH° (KJ/mol)	ΔS° (J/mol)
303	-0.38	15.721	53.15
313	-0.91		
323	-0.14		
333	-1.92		
343	-2.51		

4. Conclusion

This research focused on the synthesis and characterization of a Cu (II) coordination compound containing mixed carboxylate and nitrogen donor ligands for dye adsorption. The study aimed to contribute to the field of environmental remediation and wastewater treatment by investigating the potential of this compound as an effective dye adsorbent.

Throughout this research, a systematic approach was followed, starting with the synthesis of the Cu (II) coordination compound through a well-defined procedure. This involved the selection of suitable ligands and optimization of reaction conditions to obtain a stable and efficient adsorbent. Optimum conditions for Congo red dye adsorption were observed to be 25 mg/L dye concentration, time of 4 h, at alkaline pH, temperature of 40°C, and adsorbent dosage of 0.01 g. Equilibrium adsorption isotherms, kinetic studies, and thermodynamic analyses were performed to elucidate the adsorption behavior and mechanisms. The results indicated that the Temkin isotherm model and pseudo-second order kinetic model best-fit the adsorption data obtained in this experiment. The thermo-dynamic studies carried out showed a rapid dye removal process indicating that the [Cu(BTCA)(AMB)] adsorbent is a promising material for remediation of dye polluted water.

5. References

1. Pang Y, Zhao C, Li Y, Li Q, Bayongzhong X, Peng D, Huang T. Cadmium adsorption performance and mechanism from aqueous solution using red mud modified with amorphous MnO_2. *Sci. Rep.*, 2022, 12(1), 4424.
2. Ishak S, Rosly NZ, Abdullah AH, Alang-Ahmad SA. Fabrication of calix[4]arene/ polyurethane for the adsorptive removal of cationic dye from aqueous solutions. *Environ. Monit. Assess*., 2023, 195(11), 1303. doi: 10.1007/s10661-023-11909-z
3. Jianlong W, Xuan G. Adsorption kinetic models: physical meanings, applications, and solving methods. *J. Hazard. Mater.*, 2020., 390, 122156.
4. Holm J, Hillenbrand R, Steuber V, Bartsch U, Moos M, Lubbert H, Montag D, Schachner M. Structural features of a close homologue of L1 (CHL1) in the mouse: A new member of the L1 family of neural recognition molecules. *Eur. J. Neurosci.*, 1996, 8(8), 1613-1629.
5. Adimula VO, Elaigwu SE, Owalude SO, Clayton HS, Rotifa AA, Adeniyi E, Tella AC. Synthesis and characterization of the cu(ii)-quinoxaline, 3,3-thiodipropionate mixed ligand coordination polymer for the removal of methylene blue from aqueous solution. *Chem. Eng. Commun.*, 2024, 211(8), 1175-1190.
6. Tella AC, Bamgbose JT, Adimula VO, Omotoso M, Elaigwu SE, Olayemi VT, Odunola OA. Synthesis of metal–organic frameworks (MOFs) MIL-100(Fe) functionalized with thioglycolic acid and ethylenediamine for removal of eosin B dye

from aqueous solution. *SN Appl. Sci.*, 2021, 3(1). https://doi.org/10.1007/s42452-021-04163-w
7. Tella AC, Oladipo AC, Adimula VO et al. Synthesis and crystal structures of a copper(II) dinuclear complex and zinc(II) coordination polymers as materials for efficient oxidative desulfurization of dibenzothiophene. *New J. Chem.*, 2019, 43, 14343-14354.
8. Tella AC, Oladipo AC, Adimula VO et al. Synthesis and crystal structures of zinc(II) coordination polymers of trimethylenedipyridine (tmdp), 4-nitrobenzoic (Hnba) and 4-biphenylcarboxylic acid (Hbiphen) for adsorptive removal of methyl orange from aqueous solution. *Polyhedron*, 2020, 192, 114819.
9. Tella AC, Owalude SO, Olatunji SO et al. Synthesis of zinc-carboxylate metal-organic frameworks for the removal of emerging drug contaminant (amodiaquine) from aqueous solution. *J. Environ. Sci.*, 2018, 64, 264-275.
10. Adimula VO, Tella AC, Owalude SO, Oladipo AC, Olayemi VT, Adeniyi E, Ismail B, Mumtaz A, Khan AM. Synthesis, characterization and catalytic studies of bimetallic heteronuclear com-plexes for the reduction of nitro-aromatic compounds. *Inorg. Nano-Met. Chem.*,2022.doi: http://10.1080/24701556.2022.2078364
11. Sagita CP, Nulandaya L, Kurniawan YS. Efficient and low-cost removal of methylene blue using activated natural kaolinite material. journal of multidisciplinary. *Appl. Nat. Sci.*, 2021, 1(2), 69-77.
12. Liu Z, He W, Zhang Q, Shapour H, Bakhtari MF. Preparation of a GO/MIL-101(Fe) composite for the removal of methyl orange from aqueous solution. *ACS Omega*, 2021, 6(7), 4597-4608.
13. Ma X, Wang L, He Q, Sun Q, Yin D, Zhang Y. A review on recent developments and applications of green sorbents-based solid phase extraction techniques. *Adv. Sample Prep.*, 2023, 6, 100065.
14. Meng W, Ma Z, Shu J, Li B, Su P, Wang R, Chen M, Liu Z, Ai K. Efficient adsorption of methylene blue from aqueous solution by hydrothermal chemical modification phosphorus ore flotation tailings. *Sep. Purif. Technol.*, 2022, 281, 119496.
15. Mohammed B, Youssef M, Gulsun AE, Farid Z, Sanae L. Recent advances in adsorption kinetic models: Their application to dye types. *Arabian J. Chem.*, 2021, 14(4), 103031.
16. Mu X, Liu X, Ye X, Zhang W, Li L, Ma P, Song D. Branched poly(ethylenimine) carbon dots-MnO_2 nanosheets based fluorescent sensory system for sensing of malachite green in fish samples. *Food Chem.*, 2022, 394, 133517.
17. Munir M, Nazar MF, Zafar MN, Zubair M, Ashfaq M, Hosseini-Bandegharaei A, Khan S, Ahmad A. Effective adsorptive removal of methylene blue from water by didodecyldimethylammonium bromide-modified brown clay. *ACS Omega*, 2020, XXXX, XXX, XXX−XXX. https://dx.doi.org/10.1021/acsomega.0c01613
18. Nachiyar CV, Rakshi AD, Sandhya S, Britlin Deva Jebasta N, Nellore J.

Developments in treatment technologies of dye-containing effluent: A review. *Case Stud. Chem. Environ. Eng.*, 2023, 7, 100339. https://doi.org/10.1016/j.cscee.2023.100339.

19. Revellame ED, Fortela DL, Sharp W, Hernandez R, Zappi ME. Adsorption kinetic modeling using pseudo-first order and pseudo-second order rate laws: A review. *Cleaner Eng. Technol.*, 2020, 1, 100032. https://doi.org/10.1016/j.clet.2020.100032.
20. Rohaley GAR, Hegmann E. The importance of structure-property relationship for the designing of biomaterials using liquid crystal elastomers. *Mater. Adv.*, 2022, 3, 5725-5734.